Structural Evolution of an Interpolyelectrolyte Complex of Charged Dendrimers Interacting with Poly(L-glutamate)

Dietrich Leisner and Toyoko Imae*

Research Center for Materials Science, Nagoya University, Chikusa, Nagoya 464-8602, Japan

Received: August 22, 2003; In Final Form: November 18, 2003

The size and molecular mass of water-soluble interpolyelectrolyte complex (PEC) formed between poly(L-glutamate) and poly(amido amine) dendrimer in aqueous solution were estimated as a function of the decreasing pH from the turbidities (τ) and their wavelength dependence, by comparison with numerical τ calculations by applying the Rayleigh−Debye−Gans and Mie scattering theories. Close to the pK_a of the peripheral amino groups of the dendrimer, PECs with densities comparable to that of fractal clusters from a reaction limited colloid aggregation process collapsed to dense particles with ∼1 μm diameter. At a pH close to the pK_a of the amino groups in the interior of the dendrimer, systems with carboxylate excess over amino/ammonium groups formed compact particles, and ion pairing likely extended to the ammonium groups in the dendrimer interior. PECs with the highest polymer density were formed at the stoichiometric ratio: They appeared to be stable against dissociation at pH 3 in contrast to PECs formed with high dendrimer excess.

Introduction

Interpolyelectrolyte complex (PEC) formation in aqueous solutions is widely used[1] for separation processes (by flocculation[2] or coacervation[3]),[4] for enzyme/drug immobilization[3] and stabilization by physisorption into complex coacervates, hydrogels,[5] or microcapsules,[6,7] and for controlled drug release from pH-,[8−11] temperature-,[12] or irradiation-sensitive[13] "smart" hydrogels and capsule membranes.[12] Many of the applications require control (or proper choice) of the strength of the binding interaction, which is governed by the electrostatic energy of the correlated charge patches of the polyion (polyampholyte),[3,14] in addition to hydrophobic[15] and specific free energies (e.g., hydrogen-bonding).[16,17] The complex formation among weak polyelectrolytes is thus restricted to a pH range where the dissociation makes a "critical" minimum charge density be exceeded, which increases with the hydrophilicity of the polyion backbone and with the screening of the charges by a higher ionic strength.

The geometry and flexibility of the interacting colloids determine the shape of the PEC particles.[18] Here we consider a linear, semiflexible host polyelectrolyte (HPE, contributing more charges) interacting with an almost spherical but flexible dendrimer as guest polyelectrolyte (GPE). Such a system may form partial interpenetrating PECs, as suggested from simulation[18] and experimentally observed in a similar dendrimer/polyelectrolyte system.[19] At a sufficiently low concentration of the HPE or high GPE excess, "monomolecular" soluble PECs generally prevail.[20,21] At higher polyelectrolyte concentrations and a more balanced stoichiometric ratio, the probability of GPE cross-linking two or more HPEs increases. A series of transitions was detected (from light scattering and turbidity) between a monomolecular PEC phase and a highly aggregated PEC coacervate or precipitate in a system with a weak polyelectrolyte and spherical polycations (mixed surfactant micelles) each at a distinct pH (or charge density).[17] A PEC system with a globular

protein behaved analogously.[22] These suggest that multimolecular PECs are generally unstable against the unlimited (secondary) colloid aggregation, which after the coalescence of clusters would result in the macroscopic phase separation. The tendency to secondary aggregation was found much lower if the primary PEC colloids are more hydrophilic.[21,23]

In a recent paper[24] we have studied the formation of PEC between sodium poly(L-glutamate) and fourth generation amino-terminated poly(amido amine) (G4 PAMAM-NH2) dendrimer and its aggregation by static and dynamic light scattering (SLS and DLS). With increasing the extent of the dendrimer protonation and of the charge density on the polycation, weak interaction, soluble complex formation, PEC aggregation, and complex coacervation (at higher overall polymer concentration) were observed. The PEC aggregation occurred in a narrow pH range and followed an apparent scaling behavior with the proton activity. The hydrodynamic radius of the clusters could be well determined from the DLS data to grow up to 1300 nm. The interpretation of the SLS data in the regime of turbid aggregating clusters was highly ambiguous, due to a too limited range of scattering angles observed, and due to the possibility of multiple scattering. The turbidity data to be reported here will provide the validation or replacement of the small-angle extrapolation of the intensities in the regime of stronger light scattering from the aggregating PEC clusters. Turbidity data have the advantage to be not affected by multiple scattering and to not require extrapolation. However, their interpretation is more model-dependent than that of the angle-dependent LS data. The aim of the present study is to explore the range of soluble PEC formation in the system and to relate the evolution and transitions of the PEC structure (size, density, molecular mass) to the stoichiometry and pH-dependent charge[25] of the PECs. Special attention will be given to the possibility of different interactions with the primary amino groups in the dendrimer periphery, to be protonated at high pH, and with the tertiary amino groups in the interior of the dendrimer, which require a 300 times higher proton activity for their protonation.

* Corresponding author. Tel: +81-52-789-5911. Fax: +81-52-789-5912. E-mail: imae@nano.chem.nagoya-u.ac.jp.

Polyelectrolyte Complex with Dendrimer

J. Phys. Chem. B, Vol. 108, No. 5, 2004 **1799**

Theory

In this section we describe the obtention of modeled particle size and shape depending in the turbidity data for comparison with the experiments. In the limit of the Rayleigh–Debye–Gans (RDG) scattering approach, the turbidity coefficient, $\tau \equiv -\ln(I/I_0)/d_{slab}$, where I/I_0 is the transmission coefficient of collimated light through a slab of the scattering material of thickness d_{slab}, is given by[26]

$$\tau = c_P M_w H(\lambda_0, n_0, \mathrm{d}n/\mathrm{d}c_P) Q(R_g/\lambda) Z(R_g/\lambda, c_P) \quad (1)$$

where HQZ is an integral over the scattering angle θ of three functions: H for the total Rayleigh scattering here for unpolarized light, Q for its modification by the form factor $P_Z(\theta)$, and Z for its modification by the interparticle structure factor $S_Z(\theta)$:

$$HQZ = K_{Rayleigh} \int_{\theta_{min}}^{\pi} 2\pi \sin(\theta) \frac{1 + \cos^2(\theta)}{2} P_z(\theta) \, S_z(\theta) \, \mathrm{d}\theta \quad (2)$$

where $K_{Rayleigh}$ is an optical constant that depends on the wavelength λ_0 of the incident light in the vacuum, the refractive index of the solvent n_0, and the refractive index increment of the solute, $\mathrm{d}n/\mathrm{d}c_P$:

$$K_{Rayleigh} = \left(\frac{2\pi n_0 (\mathrm{d}n/\mathrm{d}c_P)}{\lambda_0^2}\right)^2 / N_A \quad (3)$$

N_A is Avogadro's number and θ_{min} is the acceptance angle of the detector, ideally zero. For $R_g/\lambda < 0.05$ and $S_z = Z = 1$ at solute concentration $c_P \sim 0$, $HQZ(\theta_{min}=0)$ evaluates to $K_{Rayleigh}8\pi/3$ or up to not more than 10% less, R_g being the z-averaged radius of gyration and λ being the wavelength of the light in the solution. For the initial formation of small primary PEC particles in this size limit in highly dilute solution, these conditions are approximately matched when the long-range electrostatic interactions are screened, and thus $\tau \propto M_w$ (weight-averaged molecular mass). However, for PECs becoming larger with respect to the wavelength, either by aggregation, high swelling, or anisotropic stretching, the value of QZ decreases considerably, and this decrease starts at smaller M_w for less compact particle shapes.

A spherical particle with a radius $R = (5/3)^{1/2}R_g$ has the mass $M = \rho_P(4\pi/3)R^3$, where ρ_P is the mass density of the solute in the colloid. Its form factor is[27]

$$P(u=qR) = \{3u^{-3}[\sin(u) - u\cos(u)]\}^2 \quad (4)$$

where $q = 4\pi n_0 \lambda_0^{-1} \sin(\theta/2)$ is the scalar of the scattering vector.

For a thin rodlike chain with a length $L = 12R_g$, a cylindrical cross-section of radius $R_c \ll L$, and a mass $M = \rho_P \pi R_c^2 L$, the form factor is[27]

$$P(u=qL) = \frac{2}{u}\int_0^u \frac{\sin(x)}{x}\,\mathrm{d}x - \left[\frac{2}{u}\sin\left(\frac{u}{2}\right)\right]^2 \quad (5)$$

A flexible polymer with a Gaussian coiled chain of contour length L and Kuhn segment length b has $\langle R_g^2 \rangle = bL$, $M = \rho_P \pi R_c^2 b^{-1} \langle R_g^2 \rangle$, and the form factor[27]

$$P(u=q^2\langle R_g^2\rangle) = \{2u^{-2}[\exp(-u) - 1 + u]\}^2 \quad (6)$$

Aggregating particles (e.g., branched chains of spherical beads with radius $(5/3)^{1/2}R_c$) may form clusters with mass fractal dimension d_F. In the limit $R_g > R_c$, one has $M \propto R_g^{d_F}$, and thus $M = \rho_P(4\pi/3)(5/3)^{3/2}R_c^3(R_g/R_c)^{d_F}$. In this limit the form factor is well approximated by[27]

$$P(u=qR_g) = [1 + 2u^2/(3d_F)]^{-d_F/2} \quad (7)$$

To use the models, we need consistent estimates of the parameters ρ_P, R_c, and b. Applying the "necklace" model for the PEC,[28] we take the Kuhn length $b = 4$ nm as just the diameter of a dendrimer attached to the chain, and $\langle R_c^2 \rangle^{1/2} = 1.6$ nm as an estimate for the cross-sectional radius of gyration of a fairly collapsed dendrimer bead, alternating with free thin HPE segments that contribute much less to the total scattering. Assuming that a bead of radius $(5/3)^{1/2}R_c$ accommodates a PEC domain of $M_w = 16\,673$ g/mol (14 215 g/mol for an entire GPE, plus 2458 g/mol for 16.3 monomers of the HPE), we can consistently estimate the polymer density in the bead to be $\rho_P = 750$ mg/cm^3, thus still allowing for enough water hydrating the polymer in the almost collapsed bead.

In the more general Mie scattering theory,[29] the scattering from isolated, nonabsorbing homogeneous spheres of radius R can be calculated with freely available computer programs (e.g., Mietab[30]):

$$\tau = Q_{ext}(x, n_S/n_0)c_P 3/(4R)(\mathrm{d}n/\mathrm{d}c_P)/(n_S - n_0) \quad (8)$$

where Q_{ext} is the scattering efficiency of the sphere, that is the ratio of its scattering cross-section to its geometric cross-section πR^2, and $n_S = n_0 + \rho_P(\mathrm{d}n/\mathrm{d}c_P)$ is its refractive index. As soon as the size parameter $x = 2\pi R n_0/\lambda_0$ exceeds unity, $\tau \propto R \propto M_w^{1/3}$, almost until it reaches a maximum at the first "Mie ripple", at an intermediate x which is the smaller, the larger the ratio n_S/n_0. For even larger x, $\tau(R)$ decays in a damped oscillating manner.

The above relationships can be used to calculate the turbidity of a homogenized colloidal solution as a function of wavelength, solute concentration, structure, and size of the colloids. Such calculations are shown, with parameters chosen to describe one of our experiments, in Figure 1. The ambiguity of the inverse relationship (find M_w from τ) can be reduced, when the turbidity is measured at two or more rather different wavelengths; here τ_{355} refers to the turbidity at $\lambda_0 = 355$ nm and τ_{855} to that at $\lambda_0 = 855$ nm. The turbidity ratio at two wavelengths (Figure 2) is given by the ratio of the differential volume scattering cross-sections, which does not depend on the particle concentration in the dilute solutions but depends on the particle size and shape, and which contains also the wavelength dependence of $\mathrm{d}n/\mathrm{d}c_P$ and of n_0. Nonabsorbing materials obey the Lorenz relationship $n = n_\infty(1 + a/\lambda_0^2)$ with constants, n_∞ and a, in the range of visible light. For an average globular protein in water, $\mathrm{d}n/\mathrm{d}c_P = (0.1731 + 3694 \text{ nm}^2/\lambda_0^2) \text{ cm}^3/\text{g}$.[31] Upon NaCl addition, $\mathrm{d}n/\mathrm{d}c_P$ decreases by $\cong 0.03$ M$^{-1}C_{NaCl}$.[31] For the dendrimer, we found $\mathrm{d}n/\mathrm{d}c_P \cong 0.16$ cm^3/g in 0.25 M NaCl at pH 10 and $\lambda_0 = 488$ nm. As an approximation we calculated the data in Figures 1 and 2 with a fixed $\mathrm{d}n/\mathrm{d}c_P = 0.18$ cm^3/g for the PEC and a solvent refractive index $n_0 = 1.3395$, regardless of the wavelength, for an easier recognition of the size and shape effects (HQ in eq 1, Q_{ext} in eq 8). If two of the three parameters, (i) total solute concentration, (ii) its partition between bulk and colloids, and (iii) polydispersity, can be estimated or determined with the help of other experiments, the third one can be evaluated with less ambiguity. Unfortunately, one has to consider that for large size parameters x, the main part of the scattered light will be scattered to very small angles θ. The turbidity will then be found too small, if an acceptance angle
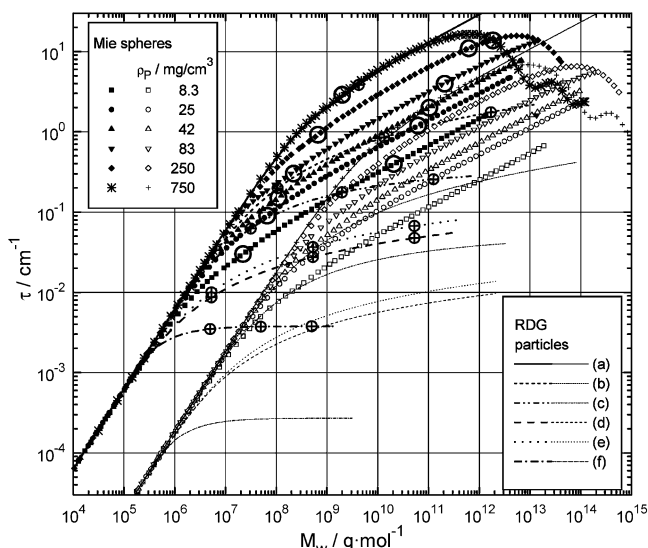
Figure 1. Modeled RDG turbidities for randomly distributed particles with $R_c = 1.7$ nm, $b = 8$ nm (coils), $dn/dc_P = 0.18$ cm^3/g, $c_P = 0.4$ mg/cm^3, $\rho_P = 750$ mg/cm^3, in solvent with $n_0 = 1.3395$, at $\lambda_0 = 355$ nm (thick lines) and 855 nm (thin lines): (a) spheres, (b) RLCA clusters ($d_F = 2.1$), (c) DLCA clusters ($d_F = 1.8$), (d) polydisperse coils, (e) monodisperse coils, (f) rods. Mie turbidities for nonabsorbing spheres are added for comparison (solid symbols, τ_{355}; hollow, τ_{855}), for different polymer densities ρ_P in the spheres. Points at which $R_g = 0.1$, 1, or 10 μm are marked with large symbols $\bigcirc$ (for Mie spheres) and $\oplus$ (for RDG particles).
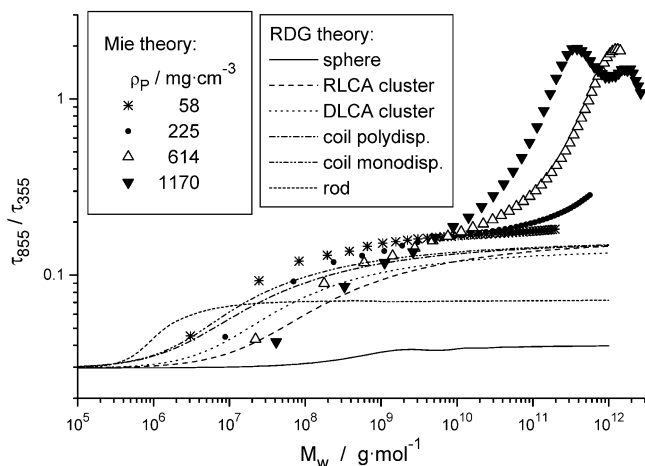
Figure 2. Calculated turbidity ratio as a function of the molecular mass and particle architecture. RDG particles are composed from spheres of radius 2.2 nm and polymer density 750 mg/cm^3. Spherical Mie particles have homogeneous polymer densities $(n_S - n_0)/(dn/dc_P)$ with $n_0 = 1.3395$ and $dn/dc_P = 0.18$ cm^3/g. The wavelength dependencies of n_0 and dn/dc_P are neglected.

$\theta_{min} > \theta$ allows many scattered photons to arrive at the detector together with the transmitted ones, which is specifically a problem, if a conventional spectrophotometer with a slit aperture to the monochromator is used (which is the case here) instead of a pinhole configuration.

Experimental Section

Materials. The amino-terminated poly(amido amine) dendrimer of the fourth generation (G4-PAMAM dendrimer, $M_w = 14.215$ kg/mol) was supplied from Aldrich Chemicals, as a 10% solution in methanol. Poly(L-glutamic acid) sodium salt (NaPGA, $M_w \sim 45$ kg/mol) was supplied from Peptide Institute Inc., lot no. 350922. Sodium chloride (NaCl) was of analytical grade. Water was distilled and further purified by a Millipore Milli-Q apparatus. Hydrochloric acid (0.25 M HCl) and sodium hydroxide (NaOH) solutions were prepared from Wako normal solutions.

Sample Preparation. Methanol was evaporated from the dendrimer solution in vacuo (about 0.1 mbar). NaPGA was dried in vacuo over silica gel prior to use. Stock solutions of the individual polymers (20 mg/cm^3 PAMAM dendrimer, 2 mg/cm^3 NaPGA) in aqueous 0.25 M NaCl and of the solvent (aqueous 0.25 M NaCl) were prepared, gently filtered through 0.22 μm Durapore membranes (Millipore Millex GV) and stored at 4−8 °C. Sample solutions were prepared by mixing these stock solutions. Hamilton syringes (50 mm^3) were used for titrations.

Measurements. All measurements were performed at 25 ± 1 °C. The pH was detected by a combined glass electrode (Iwaki, 4 mm o.d.), calibrated by standard buffers. Checking the EMF of the microsize cell after the titration for 4 h revealed a drift of the offset up to 0.15 pH units, which was taken as linear with the number of HCl additions, whereas the slope remained always unchanged. The turbidity, $\tau = -\ln(I/I_0)$, where I/I_0 is the transmission, was measured with a Shimadzu UV 2200 spectrometer in the wavelength range from 350 to 900 nm. In all titrations, the system after any addition of HCl was gently stirred and then allowed to equilibrate until a stable pH reading (usually 1 min; up to several minutes at some pHs below 6.5).

Results

An aqueous solution containing 0.2 mg/cm^3 NaPGA and 0.25 M NaCl and G4-PAMAM dendrimer at a molar excess Φ of the amino groups of the dendrimers over the carboxylate groups of the polyanions was prepared, and NaOH was added to set pH ~11, to get neutral amino groups. Then aqueous 0.25 M HCl was added stepwise. At each titration step the pH was measured potentiometrically, and the extinction was recorded as a function of the wavelength λ_0. Examples of the extinction function are shown in Figure 3. A smooth wavelength dependence indicates the absence of significant absorption bands of the PEC in the studied wavelength range, and thus virtually the extinction is due to the scattering (turbidity) only. Three different high-turbidity regimes, in general, attributable to mesoscopically or microscopically phase-separated structures were found. As a guide to the discussion, we anticipate a brief interpretation of them. The first high-turbidity regime, between pH 9 and 7, is most prominent in the cases of dendrimer excess ($\Phi > 1$) and has a rather sharp high-pH edge under these conditions. It is probably due to large PEC clusters, collapsing to particles of higher polymer density at the pH of peak turbidity. This point might indicate a charge inversion from negative to positive. In these PECs, only the protonated primary amines of the dendrimer periphery would interact with carboxylate groups from the HPE to form ion-pairs.

The second high-turbidity regime, between pH 6 and 4, is only observed in the case of HPE excess ($\Phi < 1$). In this case, PEC charge inversion is likely to occur at the broad turbidity maximum. Before this can be achieved, most tertiary amines in the dendrimer interior become also protonated ($pK_a = 6.65$)[25] and likely form ion pairs with carboxylate groups from the interpenetrating HPE, whereas the negative excess charge of HPE may be further neutralized by the beginning protonation of its carboxylate groups.

The third high-turbidity region appears in all cases as a secondary turbidity maximum or a shoulder between pH 4 and 3. It can be assigned to crystallites or fibers of PECs dominated

Polyelectrolyte Complex with Dendrimer

J. Phys. Chem. B, Vol. 108, No. 5, 2004 **1801**
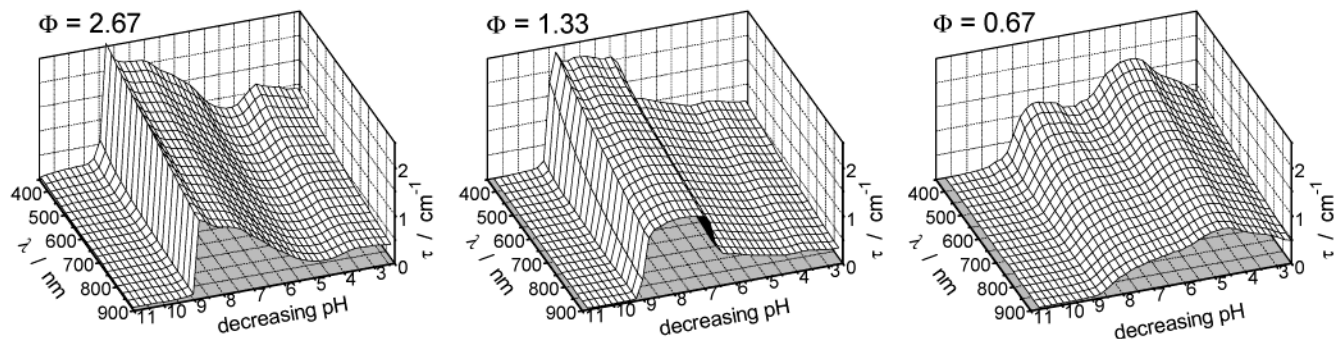
Figure 3. Turbidimetric titration of 0.2 mg/cm³ NaPGA with HCl at different G4-PAMAM dendrimer concentrations $\Phi/1.33 \times 0.2$ mg/cm³: wavelength dependence.
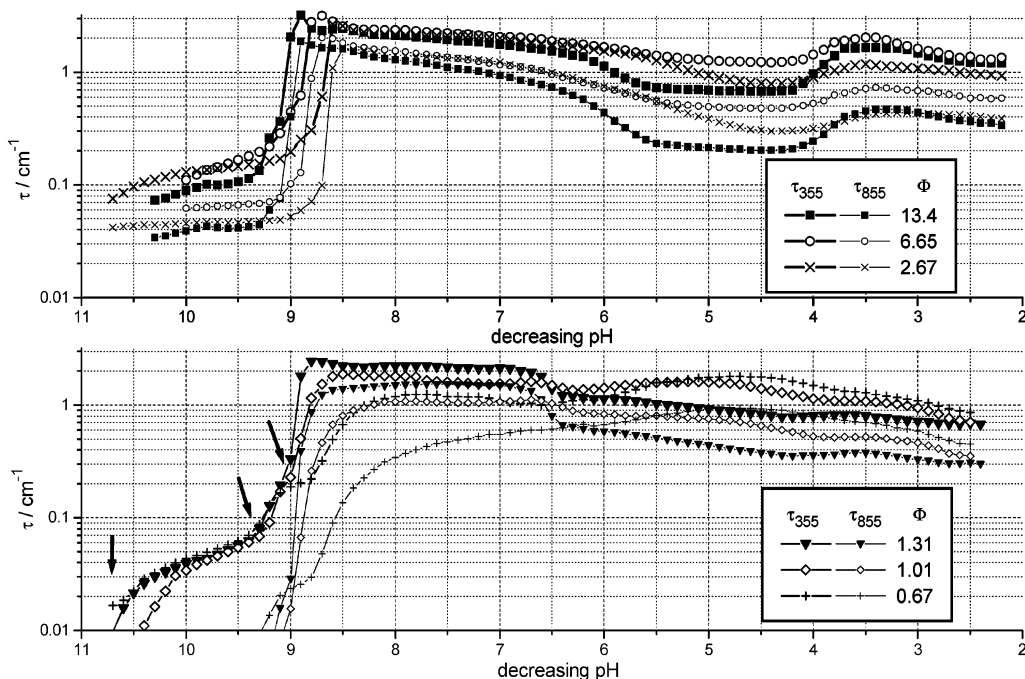
Figure 4. Turbidimetric titration of 0.2 mg/cm³ NaPGA and $\Phi/1.33 \times 0.2$ mg/cm³ G4-PAMAM dendrimer with HCl: data at two wavelengths, $\lambda_0 = 355$ and 855 nm. Arrows mark the onsets of three stages of PEC evolution upon dendrimer protonation.

by α-helical PGA domains, because the helix−coil transition[32] takes place at pH 4.2 in the absence of the dendrimer at this salt concentration,[25] when the carboxylic groups with a $pK_a =$ 4.4[25] are protonated more than 60%. The turbidity decrease at pH < 3 is due to the precipitation of a macroscopic white solid, which was not further investigated.

For the semiquantitative analysis, we focus on the turbidities at two wavelengths: τ_{355} (at $\lambda_{0,1} = 355$ nm) and τ_{855} (at $\lambda_{0,2} =$ 855 nm). Figure 4 shows these turbidities, obtained as the average of $\tau(pH,\lambda_0)$ in the wavelength range $\lambda_{0,i} \pm 5$ nm (to perform some smoothing), as a function of the pH. From Figure 1, one can see that, at the shorter wavelength, the turbidity is sensitive to the increase of the M_w in the range 10^5 to 10^{11} g/mol, covering all but the very early steps of PEC formation. On the other hand, at the longer wavelength, larger PEC clusters (up to $\sim 10^{12.5}$ g/mol) are expected to maintain a scattering yet in accord with the RDG theory, but the turbidity τ_{855} from particles with $M_w < 10^6$ g/mol cannot be distinguished from the noise at the applied colloid concentrations and slab thickness. The ratio of the turbidities, τ_{855}/τ_{355}, displayed in Figure 5, is an indicator for the type of scattering: it is close to $(\tau_{855}/\tau_{355})^{-4} \sim 0.03$ for Rayleigh scattering, is <0.16 in the RDG region, and may reach values close to unity in the "Mie ripple" region (compare with Figure 2).
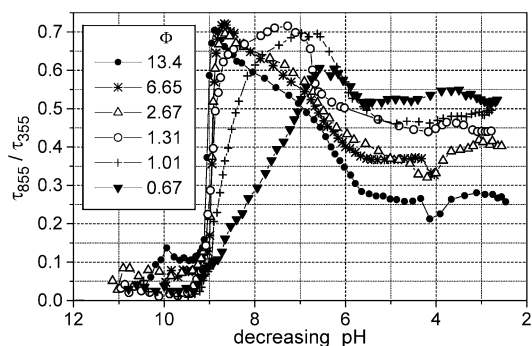
Figure 5. Wavelength dependence of measured turbidities, for different Φ.

The Rayleigh limit for small independent colloids extends only up to $\sim 10^6$ and $\sim 10^{6.7}$ g/mol at 355 and 855 nm, respectively; only in this range are the M_w calculated with eq 1 ($HQZ \cong K_{Rayleigh}8\pi/3$, $c_P = c_{NaPGA}(1 + \Phi_m)$ where $\Phi_m =$ 0.75Φ) reliable. The estimated $M_w(pH)$ are plotted in Figure 6. Larger M_w can be taken as minimum estimates, whereas $M_w <$ 5×10^5 g/mol are meaningless due to the lack of error-free baseline subtraction. First we describe the high-pH (low-turbidity) region and its evolution with the increase of the proton activity. From pH 11 to about 8.8, the turbidity (and likely the
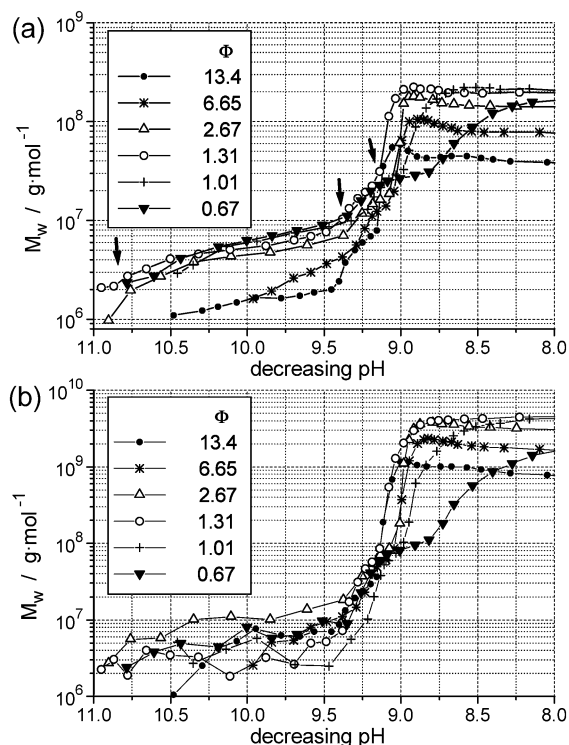
Figure 6. Conservative estimates of weight-averaged molecular mass in the mixtures from turbidities in Figures 3 and 4 and (from Rayleigh limit of RDG theory, eq 1): (a) from τ_{355}; (b) from τ_{855}. Arrows in (a) mark the onsets of three different evolution steps upon dendrimer protonation.

TABLE 1: Transitions in the Observed High-pH Turbidity Behavior upon Dendrimer Charging, as a Function of the GPE/HPE Stoichiometry[a]

Φ	pH	$\tau_{355}/$ cm^{-1}	$\tau_{855}/$ cm^{-1}	$\tau_{855}/$ τ_{355}	$M_{w,355}/$ g·mol^{-1}	$M_{w,855}/$ g·mol^{-1}
Onset (of step) 1: Transient PEC Formation						
0.67	10.78	0.017	0.001	0.030	2.9×10^6	2.9×10^6
1.01	10.45	0.025	0.001	0.052	3×10^6	6.3×10^6
1.31	10.95	0.021	0.001	0.032	2×10^6	2.8×10^6
2.67	10.90	0.014	0.001	0.084	1.2×10^6	3.4×10^6
6.65	9.96	0.048	0.002	0.047	2.0×10^6	3.1×10^6
13.4	10.48	0.060	0.002	0.029	1.4×10^6	1.3×10^6
Onset (of step) 2: Low-Density PEC Cluster Aggregation						
0.67	9.35	0.082	0.002	0.024	1.4×10^7	1.1×10^7
1.01	9.33	0.086	0.001	0.017	1.2×10^7	6.9×10^6
1.31	9.49	0.076	0.002	0.020	9.4×10^6	6.4×10^6
2.67	9.37	0.104	0.008	0.078	8.6×10^6	2.3×10^7
6.65	9.38	0.128	0.010	0.076	5.3×10^6	1.4×10^7
13.4	9.45	0.109	0.011	0.104	2.5×10^6	8.6×10^6
Onset (of step) 3: Beginning PEC Cluster Collapse						
0.67	8.82	0.230	0.025	0.107	3.8×10^7	1.4×10^8
1.01	8.95	0.446	0.049	0.109	6.3×10^7	2.3×10^8
1.31	9.14	0.310	0.025	0.081	3.9×10^7	1.0×10^8
2.67	9.08	0.274	0.038	0.137	2.3×10^7	1.0×10^8
6.65	9.10	0.416	0.054	0.130	1.7×10^7	7.6×10^7
13.4	9.16	0.430	0.059	0.138	9.7×10^6	4.5×10^7

[a] $M_{w,\lambda}/$g·mol^{-1} is the molecular mass estimate obtained from τ_λ considering Rayleigh scattering.

M_w) increases with decreasing pH in three steps. Their onsets are reported in Table 1. At pH 11, the M_w is $10^6 \pm 10^6$ g/mol, undetermined within experimental error and possibly equal to the M_w of the noninteracting PE mixtures. Starting at pH between 11.1 and 10.5 (onset 1), τ_{355} and M_w increase linearly with the decreasing pH down to pH 9.4 ± 0.1. At the end of that increase, the M_w has reached significant values between

2.5 × 10^6 and 14 × 10^6 g/mol; the higher values corresponding to the systems with no dendrimer excess. For the two highest dendrimer excesses (Φ = 13.4 and 6.65), the M_w values from τ_{355} (τ_{855}) at the end of the first increase were found to be 2.5 × 10^6 (7 × 10^6) and 5 × 10^6 (10 × 10^6) g/mol, respectively. The lowest values with respect to the other mixing ratios were indeed expected, because the excess dendrimer more dominantly contributes to the M_w and because the GPE excess decreases the probability that a GPE cross-links two HPEs.

The second step in the turbidity and corresponding M_w increase is observed in a very narrow pH range, between 9.4 ± 0.1 (onset 2) and 9.17 ± 0.05 (onset 3). In this range, which interestingly is centered at the pK_a = 9.2 of the dendrimer's primary amino groups,[25] the turbidity scales with the power 2.5 $\pm$ 0.5 of the proton activity, as can be observed from the slopes in the double logarithmic Figure 4. The normalized turbidity $\tau_{355}(0.4$ mg/cm$^3)/c_P$ at the end of that step is in the range 0.08− 0.51 cm^{-1}. These turbidities are already too large to be related to an unambiguous M_w estimate. We see in Figure 1 that 0.32 cm^{-1} is the limiting RDG turbidity $\tau_{355}(0.4$ mg/cm$^3)/c_P$ of diffusion-limited colloid aggregation (DLCA) clusters of even much higher M_w ($\geq 10^{11}$ g/mol), whereas such a turbidity could either be measured if all the solute forms RLCA clusters with $M_w = 4 \times 10^8$ g/mol and the estimated core size (R_c). The M_w estimated from τ_{855} are now more reliable than those estimated from τ_{355} and show a peak ($M_w \geq 2.3 \times 10^8$ g/mol) at the stoichiometric ratio (Φ = 1.01).

When the pH is decreased to below 9.17, in all mixtures with an excess of the dendrimer amino groups over carboxylic groups ($\Phi > 1$), the turbidity increases by about 1 order of magnitude in a pH range as narrow as 0.2. The particles obviously become too large or dense for the RDG treatment: this can be seen from the strong increase of the ratio τ_{855}/τ_{355} to ∼0.7 (Figure 5), which exceeds significantly the limit for RDG particles (0.16, see Figure 2), when the pH is lowered to below 9. Further, $M_w \geq 4 \times 10^{10}$ g/mol can be yet conservatively estimated from $\tau_{855} \geq 1.4$ for the general RDG or Mie particles, at the maximum at pH ≤ 9. The apparently highest M_w is found to be $\geq 5 \times 10^{10}$ g/mol from $\tau_{855} = 0.86$ at Φ = 1.01. In all cases the maximum of τ_{355} occurs at a significantly higher pH than that of τ_{855}, which is clear evidence for the saturation of the scattering efficiency (Mie scattering regime, first Mie ripple, accessed at a certain size/wavelength ratio, thus, for growing particles, first at smaller wavelength). Figure 1 shows that the τ_{355} at this Mie ripple should reach 18 cm^{-1}, a much higher value than the 2.6 cm^{-1} actually found. Thus either τ_{355} is measured far too low, or, more likely, less than 15% of the polymer forms large spheres with an $M_w > 10^{11}$ g/mol, which dominate the total scattering in a polydisperse system.

In the case of HPE excess ($\Phi \leq 1.01$), the transition (onset 3) is shifted to considerably lower pH values (the second high-turbidity region) and becomes much less abrupt.

In the near-stoichiometric cases, the turbidity maximum is a broad plateau ranging up to pH 6.7, a pH just above the pK_a = 6.65 of the tertiary amino groups in the interior of the GPEs. Both the turbidities and the ratio τ_{855}/τ_{355} decrease when these amino groups become protonated, and the effect is larger when the dendrimer excess Φ is increased. The most drastic change at this pK_a is at Φ = 1.31 (1:1 mass ratio), as can be seen from the strong decrease in the τ_{855}/τ_{355} in Figure 5. The response of the PEC system to produce an equilibrium pH after a HCl addition was systematically slow in this pH range and especially in the case Φ = 1.31, where considerable drift of the pH reading continued for more than 10 min. Obviously a heavily cross-

Polyelectrolyte Complex with Dendrimer

J. Phys. Chem. B, Vol. 108, No. 5, 2004 **1803**
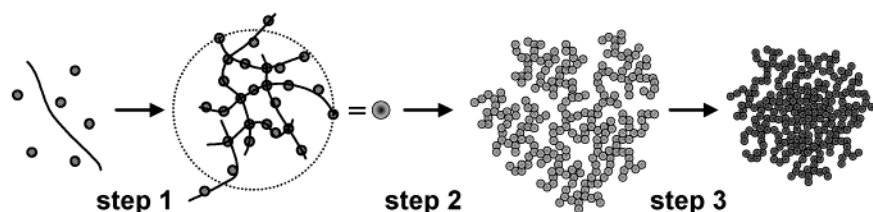
Figure 7. Schematic presentation of regimes of the transitions. A primary PEC cluster is formed at the end of step 1, which undergoes cluster aggregation to form large secondary PEC clusters at the end of step 2. In the vicinity of their isoelectric point, clusters may collapse to "spheres" in step 3.

linked, compact cluster (Mie sphere like scatterer) is forced to slowly rearrange into a more expanded structure (less dense scatterer), to distribute the PEC overcharge. The slow expansion must proceed before new protons can be rapidly accepted by the GPE.

In the range $5.5 > \text{pH} > 2.5$ the ratio τ_{855}/τ_{355} remains at high plateau values above 0.2 which are highest ($\sim$0.5) for the lowest Φ. This means that large and dense Mie scatterers remain in the system although, at a pH below the $pK_a = 4.4$ of the HPE carboxylic groups, free segments of the HPE would become more and more protonated. τ_{355} does not decrease to below 0.7 cm^{-1} in that range, with the lowest values attained at large Φ and pH just above the pK_a of the HPE. Protonating further, at pH 4 (just below the pH of the helix−coil transition of the PGA), τ_{355} and τ_{855} subsequently increase again, producing a kink in the τ_{855}/τ_{355} vs pH curves. This increase toward a turbidity maximum at pH 3.5 is more pronounced the higher is the dendrimer excess, and a dispersion of white solid is produced like in the crystallization of α-helical PGA.

Discussion

The τ vs pH behavior will be discussed first and then we will discuss the significance of the interpretation and compare the results to the outcome from static and dynamic light scattering experiments.

The first two steps of PEC growth do not depend so much on the stoichiometry but obviously on the electrostatic charge density on the dendrimer: critical charge densities for PEC formation are widely established. The first step (onset 1) was more accurately determined from static light scattering.[24] The second step probably is a colloid aggregation process between PEC clusters with positively and negatively charged patches (the peripheric GPEs and HPE segments). Because of a nonzero net charge of the clusters, the aggregation will require an additional attractive interaction, likely the increasing Flory−Huggins incompatibility between solvent molecules and growing PECs. At the beginning of the third step the turbidity is found a little larger than the expectation for DLCA clusters, but is well in the range as expected for intermediates between DLCA and RLCA clusters. A probable scenario is that, in the observed collapse transition (onset 3), such clusters of a $M_w > 10^{11}$ g/mol become nearly electroneutral (by GPE protonation) and then do not withstand a collapse of the cluster to a dense sphere with the same M_w, which might coalesce with a few further PECs. Even if the collapse occurs only for 15% of the PEC, the scattering will be dominated by that of the spheres. The collapsed fraction likely becomes maximal at the pI of the PEC. Generally, the collapsed sphere may be stabilized against aggregation by a hydrophilic corona of expanded, charged PEC. Otherwise, a complex coacervate is formed at slightly higher polymer concentration. The evolution up to this point is sketched in Figure 7. Upon further protonation, an expansion of the overcharged sphere is likely, to decrease both the turbidity and

the ratio τ_{855}/τ_{355}. But collapsed spheres, responsible for $\tau_{855}/\tau_{355} \gg 0.16$, are obviously not completely reswelled until the pH is lowered to at least the pK_a of the carboxylic functions.

PECs with $\Phi \gg 1$, which collapsed before the tertiary amines in the dendrimer interior were protonated, reswell at pH < 4. Enough PGA segments are released to become extensively protonated and to form crystalline (α-helical) domains, so that the turbidity exhibits another maximum at pH 3.5. Systems with $\Phi < 1.3$ also show such a maximum, although much less pronounced because the PECs are more stable at pH $\sim$ 5.

In static light scattering,[24] the R_g of PEC particles was found to increase with the power 0.44 of the proton activity in the first and second stages from $\sim$40 nm, to "saturate" finally at 250−500 nm, with the validity of the finding depending on the correct zero-extrapolation of the scattering curve $I(q)$. Such zero extrapolation may be very erroneous in the case of large particles, for the following reasons: (i) The scattering angle dependency of the scattering from large and dense "Mie particles" is rather different from that of RDG particles at any but the smallest (not accessed) angles. (ii) The scattering function for polydisperse nonabsorbing Mie particles at accessed scattering angles between 15 and 150° may look similar to that for polydisperse RDG particles with far lower average sizes (R_g). Details of the Mie scattering function depend strongly not only on the size parameter (e.g., R_g/λ) but also on the relative refractive indices. (iii) Multiple scattering is also a concern, which, if ignored in strongly light attenuating samples, leads to the finding of too small particles. On the other hand, turbidity measurements are not influenced by multiple scattering and do not need to rely on extrapolation. However, a nonzero acceptance angle $\theta_{\min}$ may cause underestimated turbidities at high ratios R_g/λ and thus also some too high ratios τ_{855}/τ_{355}. However, the effect should be small unless R_g reaches several μm.

Consequently, for particles with large M_w, the combination of turbidity measurement at two wavelengths and DLS yields more reliable results than the combination of "high-angle" low-resolution SLS data without special Mie fitting and DLS. The highest found values of $\tau_{855} \sim 1 \text{ cm}^{-1}$ at $c_P = 0.4$ mg/cm^3 can only be explained by dense particles with a $M_w > 2 \times 10^{10}$ g/mol; even RLCA clusters, of 1000-fold higher M_w, on the basis of dense necklace beads aggregation, would not yield such a high turbidity. The high ratio $\tau_{855}/\tau_{355} \sim 0.7$ found is further evidence of the scattering from too dense and large particles, as described by RDG theory (see Figure 2): the presence of large dense spheres ($R > 500$ nm) is most likely.

Dynamic light scattering showed[24] that a correlation length ξ_2 which was attributed to the average nonrandom distance between PEC clusters increased from 80 to 1300 nm in the case of high dendrimer excess ($\Phi \geq 2.67$) in the first and second stages, whereas in the stoichiometric case ($\Phi = 1.01$) ξ_2 increased only to 630 nm. ξ_2 was interpreted as the diameter of the average spherical cell of volume V_{cell} that makes up the depletion layer around a single PEC cluster. Considering that

all the polymer mass $V_{cell}c_P$ is accumulated in the PEC cluster in the center of V_{cell}, the corresponding cluster (molecular) mass was calculated and was found in the same order of magnitude as the M_w independently calculated from the extrapolated zero-angle scattering intensities. With the R_g of the clusters evaluated from the indirect Fourier transform of the measured static light scattering function to be in the range $45-300$ nm, the PEC cluster with spherical excluded volume $(5/3)^{3/2}R_g^3$ was estimated to consist of more than 99% of solvent. The refractive index of such a particle would be less than 0.3% different from the refractive index of the solvent. Such a particle would need a R_g larger than 5 μm to exhibit similar scattering efficiencies for lights of 355 and 855 nm wavelengths, that is, to surpass the first Mie ripple for the former. However, as indicated in Figure 1, a sphere with a refractive index 10% larger than that of the solvent, being filled with a collapsed PEC at a polymer density $\rho_P = 750$ mg/cm^3, reaches the first Mie ripple at $R_g = 600$ nm. In light of this result the former interpretation of the DLS data becomes doubtful. It is much more likely that, at least after the collapse transition, $\xi_2(q{\rightarrow}0)$ corresponds to the hydrodynamic radius R_h of the PEC cluster. For a perfect (hard) sphere, $R_h = R = (5/3)^{1/2}R_g$; thus the $\xi_2 = 1300$ nm would correspond to $R_g \sim 1000$ nm, where $\tau_{855}/\tau_{355} = 0.7$ is expected for a $\rho_P = 290$ mg/cm^3. For the stoichiometric PEC, $R_g \sim 490$ nm and the polymer density ρ_P in such spheres would be moderate 600 mg/cm^3 to match the condition $\tau_{855}/\tau_{355} = 0.7$ (see Figure 2). The previous interpretation of the light scattering data could, however, be valid in the first stages of the PEC formation still far away from the collapse transition. The light scattering data taken from that region, where $\tau_{855}/\tau_{355} < 0.15$ indicates RDG behavior, were apparently analyzed by a proper method.

Conclusions

Wavelength-dependent turbidity measurements of solutions containing bifunctional dendrimer and homopolyelectrolyte, undergoing PEC formation upon protonation of the dendrimer, revealed three high-turbidity regimes, with their pH ranges correlated with the pK_a of the concerning functional groups. The maximum of the first high-turbidity regime was close to the pK_a of the peripheral amino groups of the dendrimer, observable only in the case of dendrimer excess. Comparative RDG and Mie analyses of the turbidity, combined with previously reported dynamic light scattering data, revealed the formation of dense PEC particles with $\sim$1 μm diameter by collapse of PECs with densities comparable to that of RLCA clusters. A second high-turbidity region was centered at a pH close to the pK_a of the amino groups in the interior of the dendrimer. It was observed for systems with carboxylate excess over amino/ammonium groups and again attributable to compact particles with similar size to the former. Then ion-pairing likely extended to the ammonium groups in the dendrimer interior. PECs with the highest polymer density were formed at the stoichiometric ratio. At pH $\lesssim$ pK_a of the carboxylic groups,

where in the absence of the dendrimer the homopolyelectrolyte undergoes α-helix formation and crystallization, a white solid is also produced with large dendrimer excess but not so in systems with apparently more stable near-stoichiometric PECs.

References and Notes

(1) Kumar, M. N. V. R. *React. Funct. Polym.* **2000**, *46*, 1−27.
(2) Chen, L. A.; Carbonell, R. G.; Serad, G. A. *J. Chem. Technol. Biotechnol.* **1999**, *74*, 740−750.
(3) Xia, J.; Dubin, P. L. In *Macromolecular Complexes in Chemistry and Biology*; Dubin, P., Bock, J., Davies, R. M., Schulz, D. N., Thies, C., Eds.; Springer: Berlin, 1994; Chapter 15, pp 247−271.
(4) Dumitriu, S.; Chornet, E. *Adv. Drug Delivery Rev.* **1998**, *31*, 223−246.
(5) Zezin, A.; Rogacheva, V.; Skobeleva, V.; Kabanov, V. *Polym. Adv. Technol.* **2002**, *13*, 919−925.
(6) Adrianov, A. K.; Chen, J.; Payne, L. G. *Biomaterials* **1998**, *19*, 109−115.
(7) Burgess, D. J. In *Macromolecular Complexes in Chemistry and Biology*; Dubin, P., Bock, J., Davies, R. M., Schulz, D. N., Thies, C., Eds.; Springer: Berlin, 1994, Chapter 17, pp 285−300.
(8) Sideratou, Z.; Tsiourvas, D.; Paleos, C. M. *Langmuir* **2000**, *16*, 1766−1769.
(9) Hu, Y.; Jiang, X.; Ding, Y.; Ge, H.; Yuan, Y.; Yang, C. *Biomaterials* **2002**, *23*, 3193−3201.
(10) Jiang, H. L.; Zhu, K. J. *J. Appl. Polym. Sci.* **2001**, *80*, 1416−1425.
(11) Sakiyama, T.; Takata, H.; Toga, T.; Nakanishi, K. *J. Appl. Polym. Sci.* **2001**, *81*, 667−674.
(12) Kono, K.; Okabe, H.; Morimoto, K.; Takagishi, T. *J. Appl. Polym. Sci.* **2000**, *77*, 2703−2710.
(13) Kono, K.; Nishihara, Y.; Takagishi, T. *J. Appl. Polym. Sci.* **1995**, *56*, 707.
(14) Park, J. M.; Muhoberac, B. B.; Dubin, P. L.; Xia, J. *Macromolecules* **1992**, *25*, 290−295.
(15) Mizusaki, M.; Morishima, Y.; Dubin, P. L. *J. Phys. Chem. B* **1998**, *102*, 1908−1915.
(16) Azegami, S.; Tsuboi, A.; Izumi, T.; Hirata, M.; Dubin, P. L.; Wang, B.; Kokufuta, E. *Langmuir* **1999**, *15*, 940−947.
(17) Yoshida, K.; Dubin, P. L. *Colloids Surf. A* **1999**, *147*, 161−167.
(18) Welch, P.; Muthukumar, M. *Macromolecules* **2000**, *33*, 6159−67.
(19) Kabanov, V. A.; Zezin, A. B.; Rogacheva, V. B.; Gulyaeva, Zh. G.; Zansochova, M. F.; Joosten, J. G. H.; Brackman, J. *Macromolecules* **1999**, *32*, 1904−1909.
(20) Rigsbee, D. R.; Dubin, P. L. *Langmuir* **1996**, *12*, 1928−1929.
(21) Imae, T.; Miura, A. *J. Phys. Chem. B* **2003**, *107*, 8088−8092.
(22) Mattison, K. W.; Dubin, P. L.; Brittain, I. *J. Phys. Chem. B* **1998**, *102*, 3830−3836.
(23) Zintchenko, A.; Dautzenberg, H.; Tauer, K.; Khrenov, V. *Langmuir* **2002**, *18*, 1386-1393.
(24) Leisner, D.; Imae, T. *J. Phys. Chem. B* **2003**, *107*, 8078−8087.
(25) Leisner, D.; Imae, T. *J. Phys. Chem. B* **2003**, *107*, 13158−13167.
(26) Penders, M. H. G. M.; Vrij, A. *J. Chem. Phys.* **1990**, *93*, 3704−3711.
(27) Pedersen, J. S. *Adv. Colloid Interface Sci.* **1997**, *70*, 171−210.
(28) Minko, S.; Kiriy, A.; Gorodyska, G.; Stamm, M. *J. Am. Chem. Soc.* **2002**, *124*, 3218−3219.
(29) Bohren, C. F.; Huffman, D. R. *Absorption and Scattering of Light by Small Particles*; Wiley: New York, 1983.
(30) MieTab 6.37 for Windows 3.1, copyright 1993−1997 by August Miller.
(31) *Light Scattering from Polymer Solutions*; Huglin, M. B., Ed.; Academic Press: New York, 1972; Chapter 6.
(32) Nishio, T. *Biophys. Chem.* **1998**, *71*, 173−184.